*Genetics of Aquatic Organisms 7(3), GA688*
https://doi.org/10.4194/GA688

RESEARCH PAPER

# Targeting the Major Capsid Protein of Rock Bream Iridovirus by *Trapa Natans* Phytochemical Compounds; a Molecular Docking Approach

**Gunasekara Chathura Wikumpriya[1,*], Rajapaksha LGTG[2], Bandara BPDM[3,*], Madhuranga Walawedurage Srinith Prabhatha[1,*]**

[1]Division of Fisheries Life Science, Pukyong National University, Busan, 48513, South Korea.
[2]Korean language program, Pukyong National University, Busan 48513, South Korea.
[3]Marine Biotechnology and Bioresource Research Department, Korea Institute of Ocean Science and Technology, Yeongdo-gu, Busan 49111, South Korea.

**How to Cite**

Wikumpriya, G.C., LGTG, R., BPDM B., Prabhatha, M.W.S., (2023). Targeting the Major Capsid Protein of Rock Bream Iridovirus by *Trapa Natans* Phytochemical Compounds; A Molecular Docking Approach. *Genetics of Aquatic Organisms, 7(3), GA688*. https://doi.org/10.4194/GA688

**Article History**
Received 28 August 2023
Accepted 02 December 2023
First Online 19 December 2023

**Corresponding Author**
E-mail: cwikumpr@jbnu.ac.kr

**Keywords**
*Insilico* drug design
*Trapa natans*
$RBIV_{mcp}$
Homology modeling
ADME

## Abstract

Asian rock bream aquaculture is challenged by iridovirus, a pathogen with no effective vaccines or antiviral agents. The present study aimed to identify natural antiviral compounds from *Trapa natans*, an aquatic plant, with potential to target the activities of major capsid protein in rock bream iridovirus ($RBIV_{mcp}$). The investigation commenced by constructing a novel 3D homology structure for $RBIV_{mcp}$ using I-TASSER server, followed by refinement and validation through galaxy refiner, ModRefiner, PDBSum, ProSA, and ERRAT servers. Active binding regions of refined protein structures were employed for molecular docking simulations using PyRx and AutoDock Vina tools. Leveraging IMPPAT and PubChem servers, a total of 13 phytochemical compounds from *Trapa natans* were identified *in silico* and subjected to docking analysis against $RBIV_{mcp}$. Among them, Ellagic acid, Galactoarabinan, and Thiamine exhibited the most favorable docking scores of -5.1 kcal/mol, -6.4 kcal/mol, and -5.9 kcal/mol, respectively. Assessment of compounds' toxicity and ADME properties by Swiss-ADME and ProTox-II servers indicated their non-hepatotoxic, non-carcinogenic, non-immunotoxic, and non-mutagenic nature within environments. These findings suggest aforementioned compounds might act as promising antiviral agents against RBIV by interacting with its major capsid protein. However, *in vitro* and *in vivo* studies are essential to validate their efficacy.

## Introduction

Modern-day aquaculture practices play a key role to fulfill the growing demand for proteins. Various fish species have been cultured commercially around the world, whereas the marine captures slowly started to shrink (Brander, 2010; Naylor et al., 2021). The commercialization of aquaculture has led to the emergence of various fish diseases which heavily impacts its sustainable production. Among different disease-causing organisms, Viruses are considered a major threat to both farmed and marine fishes (Walker & Winton, 2010; Mugimba et al., 2021; Fernández Sánchez et al., 2022). The iridovirus (IRV) is one of them with the capability to infect a dynamic range of fishes including groupers, barramundi, and amberjack regardless of their age (Ito et al., 2013; Wu et al., 2013; Chuang et al., 2022). Moreover, in the Asian region, common aquaculture species such as Rock bream, Olive flounder, and Red seabream have been widely infected with iridovirus and that causes 100% cumulative mortality at high water temperatures (Sohn et al., 2000; Jung et al., 2017; Seo et al., 2020) . This double-stranded DNA virus belongs to the irdoviridae family and has the potential to survive even in adverse environmental conditions, which makes them ideal pathogens against marine organisms (Whittington et al., 2010; Subramaniam et al., 2014; Canuti et al., 2022). Apart

from the general clinical signs such as anemia, petechiae in the gills, and enlarged spleen, prolonged infections of iridovirus cause chronic lethargy, and cessation of feeding which alternatively leads to emaciation, secondary pathogenic infections and high mortalities in fish (Kurita & Nakajima, 2012). Due to the lack of evidence on vectors and disease patterns, currently, there is no effective therapeutics drug treatment to control the spread of the fish iridovirus.

In general, the structure-associated proteins are a vital part of the survival of viruses by assisting in genome assembly, encapsulation, adoption to the host environment, maturation, and also to stimulate reinfection (Ahammad et al., 2019; Galluzzi et al., 2008; Kurita & Nakajima, 2012). The Rock bream iridovirus (RBIV) genomic structure is composed of 118 open reading frames (ORF) and among them at least 14 proteins are involved in the protein modifications and host-related functions (Do et al., 2004). The RBIV major capsid protein (MCP) is the primary structural component that accounts for 45% of the total polypeptide, which helps the viral particles during the modulation of specific viral replication complexes, to the establishment of entry and exit pathways in hosts and promotes the expansion and colonization within host cells (Tidona et al., 1998; Zhou et al., 2017). The majority of fish-related iridovirus have evolutionary conserved MCP which makes it a suitable target to design drug candidates (Tidona et al., 1998; Do et al., 2004).

In recent times research has been conducted utilizing aquatic plants and their constituents to develop effective drug candidates against emerging human pathogenic viruses such as SARS CoV, HIV, and HRV (Dwevedi et al., 2016; Nag, Banerjee, et al., 2021; Rani et al., 2023). Moreover, many phytochemical compounds isolated from aquatic plants have shown drug-like properties with the potential to control viral diseases in farm animals including fish (Aljahdali et al., 2021; Islam et al., 2022). The composition of phytochemical compounds in most aquatic plants depends on their environment and, the analysis of these different plant extracts has led to the invention of successful drug compounds which are being used in different biomedical sectors today (Guo, 2017; Saxena et al., 2021; Arya et al., 2022). The *Trapa natans* (Water caltrop) is a floating aquatic plant of the genus Trapa, that belongs to the family Lythraceae and native to temperate and tropical Asian regions. Even though, the members of the genus Tarpa have been utilized in traditional and modern medicine (particularly against pathogenic infections, diarrhea, and diabetics) it is now considered a predominant invasive species in most countries due to its extensive establishment in freshwater habitats (Adkar et al., 2014; Monacelli & Wilcox, 2021). Nevertheless, in recent research, the leaf extract of *Trapa natans* has shown antibacterial and antifungal activity against Pseudomonas spp and candida spp as well as, shown antiviral activity against SARS-CoV-2 infection (Parekh & Chanda, 2007; Stoicescu et al., 2012; Farooq et al., 2023).

The identification of targeted therapeutics for the fish industries requires the selection of small bioactive molecules by investigating the activity of the targeted protein (Ziegler et al., 2013). The computational or *insilico* approaches to designing drug candidates are generally inexpensive and low time-consuming. Most of these *insilico* analysis methods can give accurate predictions against drug target proteins ( Yin et al., 2015; Aljahdali et al., 2021). Ideal phytochemical compounds against a specific target protein can be identified based on molecular docking, molecular dynamic simulations, and by assessing their interactions in different docking poses. Moreover, computational analysis of the absorption, distribution, metabolism, excretion (ADME), and toxicology properties provide data on environmental impacts and convenient application of chemical compounds (Aljahdali et al., 2021). So far, the utilization of phytochemical compounds against RBIV has not been studied, which is a necessary requirement to widen the possibility of developing effective drugs. Therefore, the present study conveys a computer-aided methodology to investigate the phytochemical compounds of *Trapa natans* as potential drug candidates against the RBIV by targeting its major capsid protein.

## Material and methods

### Sequence Retrieval and Homology Modeling Rock Bream Iridovirus Major Capsid Protein

In the present study, the representative sequence of MCP of Rock bream iridovirus (UniProt: Q6QNG4) was retrieved from the UniProtKB (https://www.uniprot.org/uniprotkb/Q6QNG4/) database accessed on 01 December 2022 (Do et al., 2005; Bateman et al., 2021). However, given that the three-dimensional (3D) structure of the MCP protein is not fully elucidated in the database, we predicted the 3D structure by a popular online web server called I-TASSER (Iterative Threading Assembly Refinement) on 02 December 2022 (Zhang, 2008). The I- TASSER server predicted five models for the Rock bream iridovirus major capsid protein sequence (hereafter $RBIV_{mcp}$) and provided values associated with the C score, Root-mean-square deviation (RMSD), and TM-score. Based on the server suggestion higher C-score indicate a protein model has the highest confidence from positive to negative values. Hence, among the produced models, the top 3D model was selected and downloaded in PDB format considering its C-score value.

### Model Refinement and Validation

The primary and secondary refinements of the constructed 3D model were carried out by ModRefiner (https://zhanggroup.org/ModRefiner/) and Galaxy refine (https://galaxy.seoklab.org/cgi-bin/submit.cgi?type=REFINE) servers on 04 December 2022 respectively

(Xu & Zhang, 2011; Heo et al., 2013). The refined structures were downloaded and among them, the most suitable 3D structure was selected based on maximum and minimum RMSD values, the average distance between atoms, the energy score, GDT-HA, MolProbity, clash scores, and poor rotamer values. The 3D model visualization software PyMol v2.3.4 was used to visualize the final refined structure and the validation of the refined $RBIV_{mcp}$ was carried out by Ramachandran plots developed through PDBsum (http://www.ebi.ac.uk/thornton-srv/databases/pdbsum/Generate.html) web server (Laskowski et al., 2018; Aljahdali et al., 2021). Furthermore, the quality of the protein model was assessed using Z-score and quality score values by submitting it to ProSA- (https://prosa.services.came.sbg.ac.at/prosa.php) and ERRAT (https://www.doe-mbi.ucla.edu/errat/) web servers on 7 December 2022 (Colovos & Yeates, 1993; Wiederstein & Sippl, 2007).

**Protein and Ligand Preparation**

Before the establishment of a docking protocol, validated protein structures need to be modified using various bioinformatics tools. Therefore, in the present study, the $RBIV_{mcp}$ 3D structure was modified using AutoDockTools (ADT). As the Initial step gasteiger charges were calculated and non-polar hydrogen was added to the $RBIV_{mcp}$. To obtain the phytochemical compounds of interest (ligands), the Indian Medicinal Plants, Phytochemistry, and Therapeutics (IMPPAT) (https://cb.imsc.res.in/imppat/home) database was searched using the keyword "*Trapa natans*" followed by the validation with PubChem (https://pubchem.ncbi.nlm.nih.gov/) database (Mohanraj et al., 2018; Kim et al., 2021). Based on both databases a total of 13 natural chemical compounds were downloaded on 6 December 2022.

**The Protein Active site Identification and Receptor Grid Generation**

The refined $RBIV_{mcp}$ structure was submitted to CASTp 3.0 (Computed Atlas of Surface Topography of proteins) web server (http://sts.bioe.uic.edu/) accessed on 07 December 2022 (Tian et al., 2018). This server can predict different active pocket regions for a given protein with its pocket surface area (SA). In the present study, based on the active pocket surface area, the first active pocket of $RBIV_{mcp}$ was selected as the potential site for molecular docking. Moreover, the binding site residues of the active pocket region of $RBIV_{mcp}$ were visualized through BIOVIA discovery studio visualizer tool 16.1.0.

**Docking Simulation**

The popular software called "PyRx" was utilized for molecular docking simulation between $RBIV_{mcp}$ and the selected ligand compounds (Dallakyan & Olson, 2015). In modern scientific research, this software is widely applied for the virtual screening of molecular compounds-protein interaction studies, and, numerous potential drugs have been identified against veterinary diseases through various in-house protocols. The software contains both AutoDock and AutoDock Vina plugins for molecular docking along with the Lamarckian genetic algorithm (LGA) as the scoring function. In the present study, molecular docking simulations were conducted by utilizing AutoDock Vina plugin embedded in PyRx tools. The molecular complex binding poses for $RBIV_{mcp}$-ligands were visualized by BIOVIA discovery studio visualizer Tool 16.1.0.

**ADME Analysis**

If a molecular compound is to be used as a successful drug candidate it should possess different key features. These key features are called ADME or Absorption, Distribution, Metabolism, and Excretion properties, which investigates how a chemical behaves inside a living organism (Lin et al., 2003). Early confirmation of ADME properties is an indispensable part of modern drug design process research to overcome the failures of drug development and preclinical stages. When considering the application of drug candidates to Fish, the most important internal impacts are associated with physiochemical properties, hydrophobicity, gastrointestinal environment (GI), and lipophilicity (Hadni & Elhallaoui, 2020; Aljahdali et al., 2021). Hence in the present study, The ADME profiles for ligand compounds such as solubility profile, bioavailability, and GI absorption were evaluated using a free accessible server at Swiss-ADME (http://www.swissadme.ch/) for the selected compounds accessed on 11 December 2022 (Daina et al., 2017).

**Toxicity Analysis**

Before using any chemical compound, its safety needs to be evaluated and, these evaluations carry the utmost importance in preventing harmful effects on humans and animals. In recent times *insilico* computational approaches have been utilized by researchers to measure the potential toxicities of chemical compounds to develop optimum usage protocols. In the present study, ProTox-II (https://tox-new.charite.de/for) webserver was utilized to assess the toxicity of selected ligand compounds accessed on 12 December 2022 (Banerjee et al., 2018). Based on the server prediction, qualitative and qualitative approaches were used to develop a toxicity profile along with carcinogenicity, mutagenicity, and immunotoxicity values.

## Results

### Homology Modeling, Refinement, and Validation of the Tertiary Structure

The retrieved RBIV$_{mcp}$ (453 amino acid length) was submitted to I TASSER protein modeling server. Among the top 5 protein models produced, the 3D model which had highest C score (0.28), TM-score (0.75±0.10), and RMSD (6.5±3.9Å) was selected as the potential candidate and downloaded in PDB format. Before the refinement, Ramachandran plot produced through PDBsum server showed a total of 86.2%, 12.5%, and 1.3% residues in the favorable, allowed, and disallowed regions (Supplementary file 1). To improve the quality of the model, 2-step refinement was carried out by using Galaxy refiner and ModRefiner servers. The initial and secondary refinements through these servers provided a total of 5 models with GDT-HA, RMSD, MolProbity, Clash scores, and poor rotamer values ranging from 0.9801-0.9857, 0.31-0.334, 1.906-2.613, 14.7-16.5 and 0-0.5 for each parameter respectively (Supplementary file 2). Among them, model-2 was selected as the best model, indicated by the following parameters: GDT-HA (0.9857), RMSD (0.334), MolProbity (1.916), clash score (14.7), poor rotamers (0.5), and Rama favored region (97.8). Again, the validation of this refined model was conducted with PDBsum server and it showed the improved 3D model had a total of 90%, 8.6%, and 1.4% residues in the favorable, allowed, and disallowed regions in the Ramachandran plots (Figure 1). To further ensure the quality of the refined model, ProSA server and ERRAT servers were utilized. The results showed a Z-score of -6.26 and a total quality factor of 90.21 for ProSA and ERRAT server analysis, indicating it has high structural properties.

### Ligands and Protein Preparation

The phytochemical compounds (as ligands) representing *Trapa natans* were retrieved from the IMPPAT database in 2D (SDF) format (Supplementary file 3). The selected compounds were optimized during the ligand preparation steps and converted to pdbqt format. The designed models were processed for the molecular docking studies using Auto dock tools and saved in pdbqt format for further evaluation as described elsewhere (Aljahdali et al., 2021).

### Determination of Active Pocket Site, Its Homogeneity, and Receptor Grid Box Generation

The active pocket site (APS) of a certain protein is formed by the combination of different amino acid residues into a binding site region that has the capacity to make temporary bonds with the other molecules. In general, these type of APS in a protein also helps to stabilize the reaction intermediates. In this study, APS of the RBIV$_{mcp}$ was identified from CASTp server and the first binding pocket with a 484Å$^2$ was selected as the potential site for the ligand binding (Figure 2). Following, a blast search was conducted using the RBIV$_{mcp}$ to decipher the homogeneity of the active pocket region. The first 10 aligned sequences with 0 E-value and a length of 453 residues were then visualized using the MEGA software (Supplementary file 4). The data suggested that the active pock region residues of ALA7, ASN8, SER11, GLY12, VAL41, ARG42, SER43, SER44, TYR46, TYR76, ASP181, THR182, GLY183, LEU184, ALA185, ALA245, GLU251, VAL254, VAL255, SER258, SER259, ARG260, ARG261, MET262, LEU263, and ILE385 are highly conserved in other iridovirus major capsid proteins (Figure 3). Following this confirmation, a grid

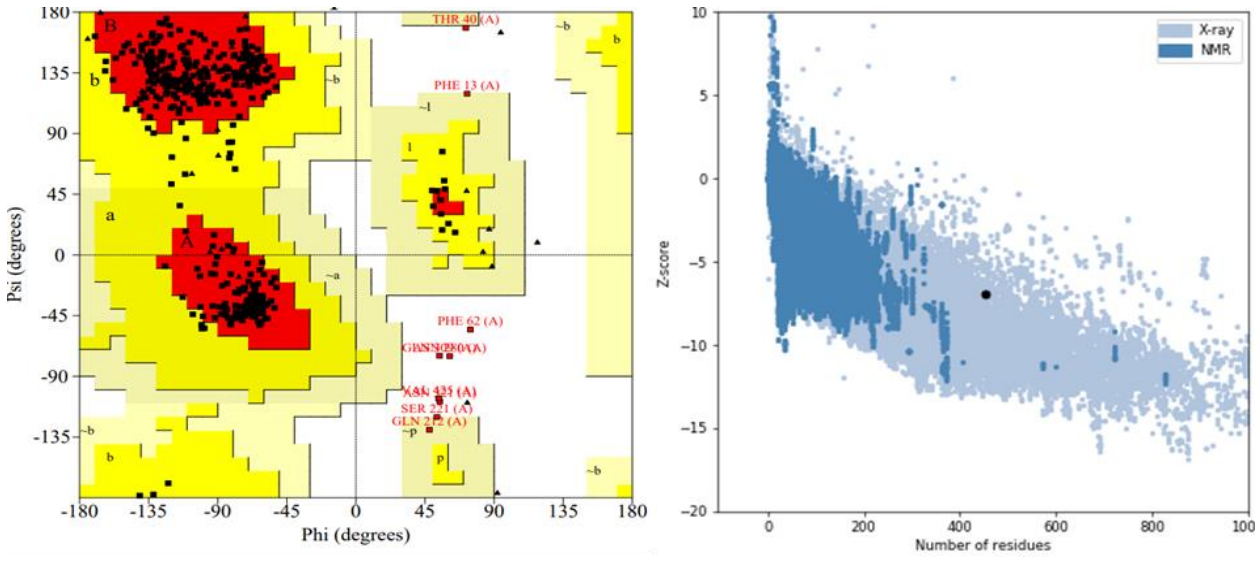


**Figure 1.** Validation of the 3D structure of the RBIV$_{mcp}$. (A) The Ramachandran plot statistics represent the most favorable, allowed, disallowed regions with a percentage of 90%, 8.6% and 1.4%, respectively, and (B) the ProSA plot with Z-score (−6.29) of refined RBIV$_{mcp}$.

box was generated with the dimensions of X=91.39, Y=48.45, and Z=53.14 in angstrom (Å) by utilizing the conserved active pocket region.

**Molecular Docking Simulation**

To identify the possible relationships between ligand compounds and the $RBIV_{mcp,}$ a molecular docking process was established. A total of 13 ligand compounds were docked using the PyRx tools plugin AutoDock Vina wizard. Upon molecular docking, ligand compounds showed binding affinities ranging from -7.7 kcal/mol to -4 kcal/mol. Among them, the compounds which had binding affinities above -5 kcal/mol were considered potential drug candidates for further analysis (Supplementary file 5). However, some of the ligand compounds had unacceptable donor-donor relationships and a low number of bonds with $RBIV_{mcp}$. After shortlisting all the above, 3 ligands namely CCID1130 (IMPHY000005), CCID5281855 (IMPHY005537), and CCID24847856 (IMPHY003230) with binding affinities of -5.1, -6.4, and -5.9 kcal/mol were extracted. Additionally, the redocking was conducted for 3 selected ligand compounds in the same binding pose which provided the almost similar binding score to the previous values (CCID1130, CCID5281855, and CCID24847856 with binding affinities -5.1.9, -6.5 and -5.9 kcal/mol).

**Protein-ligand Interaction Analysis**

The $RBIV_{mcp}$ along with the 3 docked ligand compounds were retrieved using the PyRx tools in PDBQT format. The first investigated docked ligand compound was a pyridine alkaloid called “thiamine” (CCID1130) and it had a single hydrogen bond in the residual position of GLU251 and 5 hydrophobic bonds in TYR46, TYR76, ALA245 and LEU247 of $RBIV_{mcp}$. Moreover, the binding positions, bond types, and relative distances are shown in Figure 4 and Table 1.

The second selected ligand compound was a phenolic acid called “Ellagic acid” (CCID5281855). The docking analysis showed a total of 3 hydrogen bonding interactions in the ALA185 and SER44 amino acid residues. There were 2 electrostatic bonds in GLU251 and 3 hydrophobic bonds in TYR76, and TYR46 residual positions as indicated in Figure 5. Moreover, the specific bond types and relative distances between the CCID24847856 and $RBIV_{mcp}$ are shown in Table 1.

The final ligand compound was a polysaccharide called galactoarabinan (CCID24847856). Interestingly all the bonds formed by this compound with $RBIV_{mcp}$ were hydrogen bonds in the GLU251, ARG260, GLY183, and THR182 residual positions. This polysaccharide compound had the highest number of binding relativeness compared to the other selected ligands in the study. Moreover, the specific interaction types and relative distances between the CCID24847856 and $RBIV_{mcp}$ are shown in Figure 6 and Table 1.

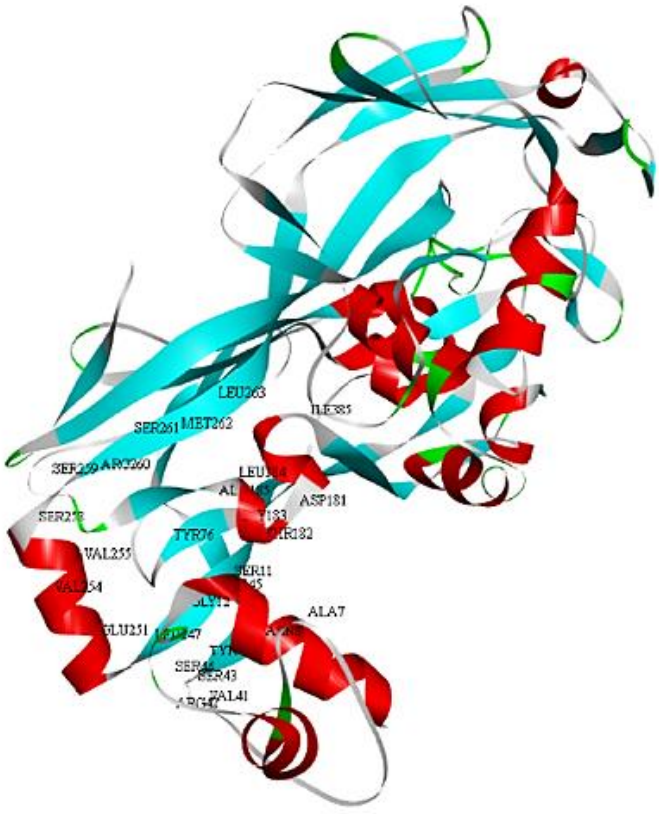


**Figure 2.** The active pocket site (APS) of $RBIV_{mcp}$ 3D structure. There was a total of 26 amino acids in the APS as indicated in black color.

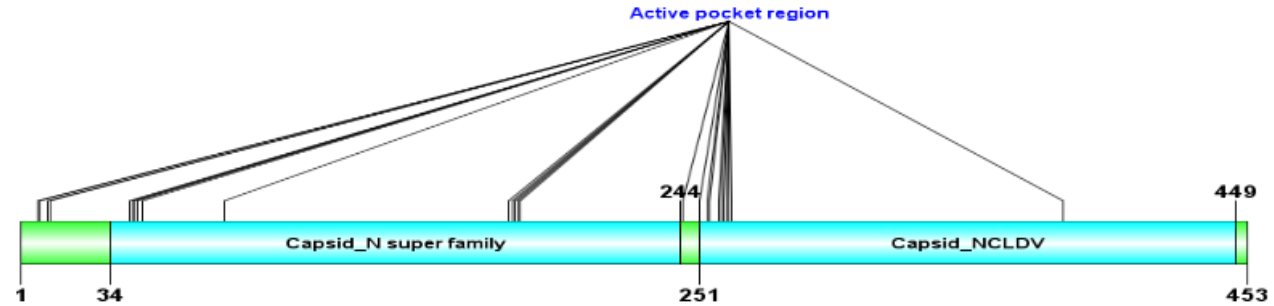


```
AAS44554.1   MSAISGANVTSGFIDISAFDAMETHLYGGDNAVTYFARETVRSSWYSKLPVTLSKQTGHANFGQEFSVTVARGGDYLINV 80
ACF54642.1   MSAISGANVTSGFIDISAFDAMETHLYGGDNAVTYFARETVRSSWYSKLPVTLSKQTGHANFGQEFSVTVARGGDYLINV 80
AAP37443.1   MSAISGANVTSGFIDISAFDAMETHLYGGDNAVTYFARETVRSSWYSKLPVTLSKQTGHANFGQEFSVTVARGGDYLINV 80
ADU25255.1   MSAISGANVTSGFIDISAFDAMETHLYGGDNAVTYFARETVRSSWYSKLPVTLSKQTGHANFGQEFSVTVARGGDYLINV 80
AAP74204.1   MSAISGANVTSGFIDISAFDAMETHLYGGDNAVTYFARETVRSSWYSKLPVTLSKQTGHANFGQEFSVTVARGGDYLINV 80
ADZ72844.1   MSAISGANVTSGFIDISAFDAMETHLYGGDNAVTYFARETVRSSWYSKLPVTLSKQTGHANFGQEFSVTVARGGDYLINV 80
AAX93516.1   MSAISGANVTSGFIDISAFDAMETHLYGGDNAVTYFARETVRSSWYSKLPVTLSKQTGHANFGQEFSVTVARGGDYLINV 80
AEI85905.1   MSAISGANVTSGFIDISAFDAMETHLYGGDNAVTYFARETVRSSWYSKLPVTLSKQTGHANFGQEFSVTVARGGDYLINV 80
QBL98278.1   MSAISGANVTSGFIDISAFDAMETHLYGGDNAVTYFARETVRSSWYSKLPVTLSKQTGHANFGQEFSVTVARGGDYLINV 80
                   **  **                        **** *                          *

AAS44554.1   WLRVKIPSITSSKENSYIRWCDNLMHNLVEEVSVSFNDLVAQTLTSEFLDFWNACMMPGSKQSGYNKMIGMRSDLVGGIT 160
ACF54642.1   WLRVKIPSITSSKENSYIRWCDNLMHNLVEEVSVSFNDLVAQTLTSEFLDFWNACMMPGSKQSGYNKMIGMRSDLVGGIT 160
AAP37443.1   WLRVKIPSITSSKENSYIRWCDNLMHNLVEEVSVSFNDLVAQTLTSEFLDFWNACMMPGSKQSGYNKMIGMRSDLVGGIT 160
ADU25255.1   WLRVKIPSITSSKENSYIRWCDNLMHNLVEEVSVSFNDLVAQTLTSEFLDFWNACMMPGSKQSGYNKMIGMRSDLVGGIT 160
AAP74204.1   WLRVKIPSTTSSKENSYIRWCDNLMHNLVEEVSVSFNDLVAQTLTSEFLDFWNACMMPGSKQSGYNKMIGMRSDLVGGIT 160
ADZ72844.1   WLRVKIPSITSSKENSYIRWCDNLMHNLVEEVSVSFNDLVAQTLTSEFLDFWNACMMPGSKQSGYNKMIGMRSDLVGGIT 160
AAX93516.1   WLRVKIPSITSSKENSYIRWCDNLMHNLVEEVSVSFNDLVAQTLTSEFLDFWNACMMPGSKQSGYNKMIGMRSDLVGGIT 160
AEI85905.1   WLRVKIPSITSSKENSYIRWCDNLMHNLVEEVSVSFNDLVAQTLTSEFLDFWNACMMPGSKQSGYNKMIGMRSDLVGGIT 160
QBL98278.1   WLRVKIPSITSSKENSYIRWCDNLMHNLVEEVSVSFNDLVAQTLTSEFLDFWNACMMPGSKQSGYNKMIGMRSDLVSGIT 160

AAS44554.1   NGQTMPAAYLNLPIPLFFTRDTGLALPTVSLPYNEVRIHFKLRRWEDLLISQSTQAELAISTVTLANIAKVAPALTNVSV 240
ACF54642.1   NGQTMPAAYLNLPIPLFFTRDTGLALPTVSLPYNEVRIHFKLRRWEDLLISQSTQADMAISTVTLANIGNVAPALTNVSV 240
AAP37443.1   NGQTMPAAYLNLPIPLFFTRDTGLALPTVSLPYNEVRIHFKLRRWEDLLISQSTQADMAISTVTLANIGNVAPALTNVSV 240
ADU25255.1   NGQTMPAAYLNLPIPLFFTRDTGLALPTVSLPYNEVRIHFKLRRWEDLLISQSTQADMAISTVTLANIGNVAPALTNVSV 240
AAP74204.1   NGQTMPAAYLNLPIPLFFTRDTGLALPTVSLPYNEVRIHFKLRRWEDLLISQSTQADMAISTVTLANIGNVAPALTNVSV 240
ADZ72844.1   NGQTMPAAYLNLPIPLFFTRDTGLALPTVSLPYNEVRIHFKLRRWEDLLISQSTQADMAISTVTLANIGNVAPALTNVSV 240
AAX93516.1   NGQTMPAAYLNLPIPLFFTRDTGLALPTVSLPYNEVRIHFKLRRWEDLLISQSTQADMAISTVTVANIGNVTPALTNVSV 240
AEI85905.1   NGQTMPAAYLNLPIPLFFTRDTGLALRTVSLPYNEVRIHFKLRRWEDLLISQSTQADMAISTVTLANIGNVAPALTNVSV 240
QBL98278.1   NGQTMPAAYLNLPIPLFFTRDTGLALPTVSLPYNEVRIHFKLRRWEDLLISQSTQADMAISTVTVANIGNVTPALTNVSV 240
                           *****

AAS44554.1   MGTYAVLTSEEREVVAQSSRSMLIEQCQVAPRVPVTPVDISLVHLDLRFSHLVKALFFAVKNVTHRNVQSNYTAASPVYV 320
ACF54642.1   MGTYAVLTSEEREVVAQSSRSMLIEQCQVAPRVPVTPVDDSLVHLDLRFSHPVKALFFAVKNVTHRNVQSNYTAASPVYV 320
AAP37443.1   MGTYAVLTSEEREVVAQSSRSMLIEQCQVAPRVPVTPVDNSLVHLDLRFSHPVKALFFAVKNVTHRNVQSNYTAASPVYV 320
ADU25255.1   MGTYAVLTSEEREVVAQSSRSMLIEQCQVAPRVPVTPVDNSLVHLDLRFSHPVKALFFAVKNVTHRNVQSNYTAASPVYV 320
AAP74204.1   MGTYAVLTSEEREVVAQSSRSMLIEQCQVAPRVPVTPVDNSLVHLDLRFSHPVKALFFAVKNVTHRNVQSNYTAASPVYV 320
ADZ72844.1   MGTYAVLTSEEREVVAQSSRSMLIEQCQVAPRVPVTPVDNSLVHLDLRFSHPVKALFFAVKNVTHRNVQSNYTAASPVYV 320
AAX93516.1   MGTYAVLTSEEREVVAQSSRSMLIEQCQVAPRVPVTPVDNSLVHLDLRFSHPVKALFFAVKNVTHRNVQSNYTAASPVYV 320
AEI85905.1   MGTYAVLTSEEREVVAQSSRSMLIEQCQVAPRVPVTPVDNSLVHLDLRFSHPVKALFFAVKNVTHRNVQSNYTAASPVYV 320
QBL98278.1   MGTYAVLTSEEREVVAQSSRSMLIEQCQVAPRVPVTPADNSLVHLDLRFSHPVKALFFAVKNVTHRNVQSNYTAASPVYV 320
                  *     *  **  ******

AAS44554.1   NNKVNLPLLATNPLSEVSLIYENTPRLHQMGVDYFTSVDPYYFAPSMPEMDGVMTYCYTLDMGNINPMGSTNYGRLSNVT 400
ACF54642.1   NNKVNLPLLATNPLSEVSLIYENTPRLHQMGVDYFTSVDPYYFAPSMPEMDGVMTYCYTLDMGNINPMGSTNYGRLSNVT 400
AAP37443.1   NNKVNLPLLATNPLSEVSLIYENTPRLHQMGVDYFTSVDPYYFAPSMPEMDGVMTYCYTLDMGNINPMGSTNYGRLSNVT 400
ADU25255.1   NNKVNLPLLATNPLSEVSLIYENTPRLHQMGVDYFTSVDPYYFAPSMPEMDGVMTYCYTLDMGNINPMGSTNYGRLSNVT 400
AAP74204.1   NNKVNLPLLATNPLSEVSLIYENTPRLHQMGVDYFTSVDPYYFAPSMPEMDGVMTYCYTLDMGNINPMGSTNYGRLSNVT 400
ADZ72844.1   NNKVNLPLLATNPLSEVSLIYENTPRLHQMGVDYFTSVDPYYFAPSMPEMDGVMTYCYTLDMGNINPMGSTNYGRLSNVT 400
AAX93516.1   NNKVNLPLLATNPLSEVSLIYENTPRLHQMGVDYFTSVDPYYFAPSMPEMDGVMTYCYTLDMGNINPMGSTNYGRLSNVT 400
AEI85905.1   NNKVNLPLLATNPLSEVSLIYENTPRLHQMGVDYFTSVDPYYFAPSMPEMDGVMTYCYTLDMGNINPMGSTNYGRLSNVT 400
QBL98278.1   NNKVNLPLLATNPLSEVSLIYENTPRLHQMGVDYFTSVDPYYFAPSMPEMDGVMTYCYTLDMGNINPMGSTNYGRLSNVT 400
                                                                        *

AAS44554.1   LSCKVSDNAKTTAAGGGGNGTGYTVAQKFELVVIAVNHNIMKIADGAAGFPIL 453
ACF54642.1   LSCKVSDNAKTTAAGGGGNGTGYTVAQKFELVVIAVNHNIMKIADGAAGFPIL 453
AAP37443.1   LSCKVSDNAKTTAAGGGGNGTGYTVAQKFELVVIAVNHNIMKIADGAAGFPIL 453
ADU25255.1   LSCKVSDNAKTTAAGGGGNGTGYTVAQKFELVVIAVNHNIMKIADGAAGFPI- 452
AAP74204.1   LSCKVSDNAKTTAAGGGGNGTGYTVAQKFELVVIAVNHNIMKIADGAAGFPIL 453
ADZ72844.1   LSCKVSDNAKTTAAGGGGNGTGYTVAQKFELVVIAVNHNIMKIADGAAGFPIL 453
AAX93516.1   LSCKVSDNAKTTAAGGGGNGTGYTVAQKFELVVIAVNHNIMKIADGAAGFPIL 453
AEI85905.1   LSCKVSDNAKTTAAGGGGNGTGYTVAQKFELVVIAVNHNIMKIADGAAGFPIL 453
QBL98278.1   LSCKVSDNAKTTAAGGGGNGTGYTVAQKFELVVIAVNHNIMKIADGAAGFPIL 453
```

**Figure 3.** MEGA alignment of the conserved active pocket site (APS) among fish iridovirus (Rock bream iridovirus-AAS44554.1, Barramundi perch iridovirus-ACF54642.1, Grouper sleepy disease iridovirus-AAP37443.1, Infectious spleen and kidney necrosis virus-ADU25255.1, Red seabream iridovirus-AAP74204.1, Stone flounder iridovirus-ADZ72844.1, Large yellow croaker iridovirus-AAX93516.1, Giant seaperch iridovirus-AEI85905.1, Seabass iridovirus-QBL98278.1) The red color indicates the APS region in the alignment.

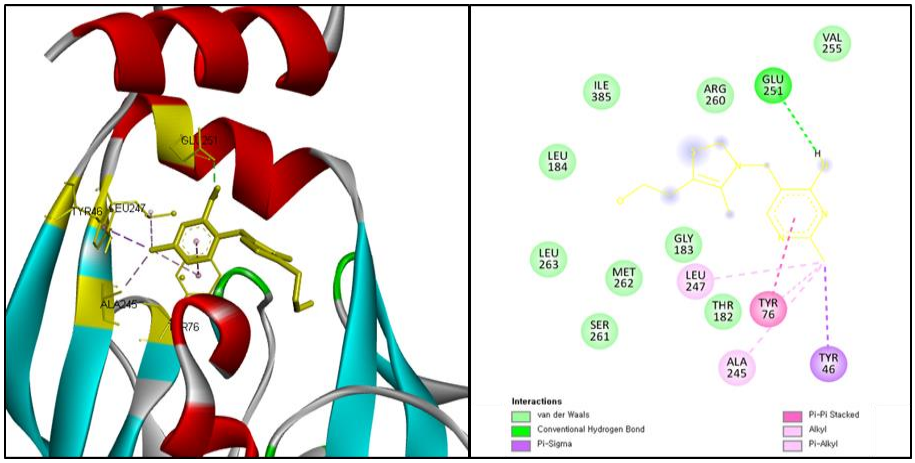


**Figure 4.** The interaction between the ligand CCID1130 and $RBIV_{mcp}$. Left side indicate 3D interaction and the right portion indicates 2D interaction of the protein -ligand complex.

**Table 1.** List of bonding interactions between selected ligand compounds with $RBIV_{mcp}$

| LIGAND | NAME | DISTANCE | CATEGORY | TYPE |
|---|---|---|---|---|
| **THIAMINE (CCID1130)** | GLU251 | 2.57301 | Hydrogen bond | Conventional hydrogen bond |
| | TYR46 | 3.93112 | Hydrophobic | Pi-Sigma |
| | TYR76 | 4.35635 | Hydrophobic | Pi-Pi Stacked |
| | ALA245 | 3.8838 | Hydrophobic | Alkyl |
| | LEU247 | 4.94253 | Hydrophobic | Alkyl |
| | TYR76 | 4.52535 | Hydrophobic | Pi-Alkyl |
| **GALACTOARABINAN (CCID24847856)** | ARG260 | 2.60062 | Hydrogen bond | Conventional hydrogen bond |
| | ARG260 | 1.83892 | Hydrogen bond | Conventional hydrogen bond |
| | ARG260 | 3.07328 | Hydrogen bond | Conventional hydrogen bond |
| | THR182 | 2.6741 | Hydrogen bond | Conventional hydrogen bond |
| | GLU251 | 2.24243 | Hydrogen bond | Conventional hydrogen bond |
| | GLU251 | 2.37183 | Hydrogen bond | Conventional hydrogen bond |
| | GLY183 | 3.49454 | Hydrogen bond | Carbon hydrogen bond |
| | GLY183 | 3.58282 | Hydrogen bond | Carbon hydrogen bond |
| | GLY183 | 3.55175 | Hydrogen bond | Carbon hydrogen bond |
| | GLY183 | 3.53438 | Hydrogen bond | Carbon hydrogen bond |
| **ELLAGIC ACID (CCID5281855)** | ALA185 | 3.09456 | Hydrogen bond | Conventional hydrogen bond |
| | ALA185 | 2.93086 | Hydrogen bond | Conventional hydrogen bond |
| | SER44 | 2.44617 | Hydrogen bond | Conventional hydrogen bond |
| | GLU251 | 4.91833 | Electrostatic | Pi-Anion |
| | GLU251 | 4.22184 | Electrostatic | Pi-Anion |
| | TYR76 | 5.41715 | Hydrophobic | Pi-Pi Stacked |
| | TYR76 | 4.41488 | Hydrophobic | Pi-Pi Stacked |
| | TYR46 | 4.92922 | Hydrophobic | Pi-Pi T-shaped |

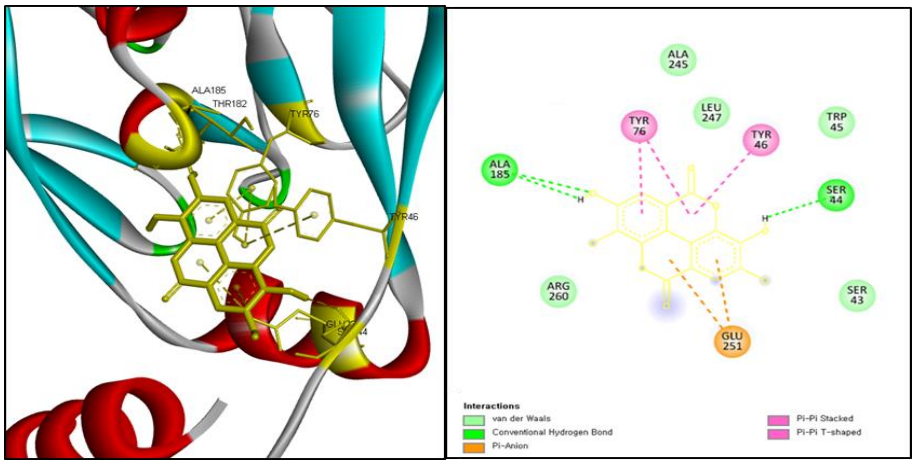


**Figure 5.** The interaction between the ligand compound CCID5281855 and $RBIV_{mcp}$. Left side indicate 3D interaction and the right portion indicates 2D interaction of the protein -ligands complex.

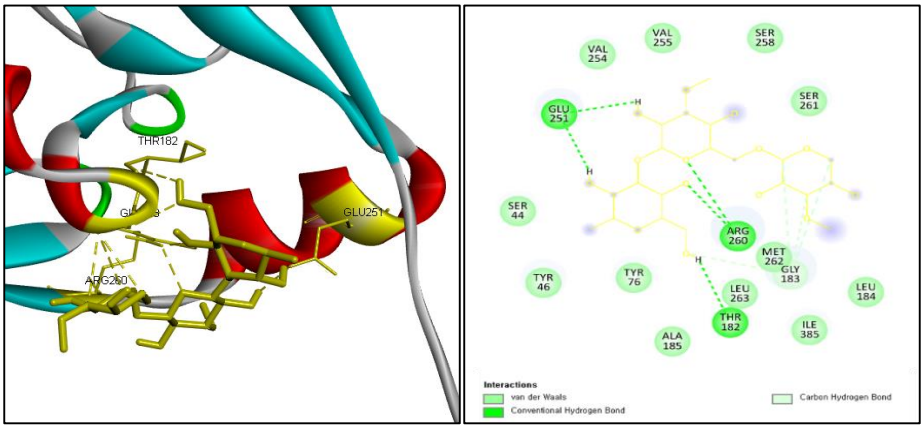


**Figure 6.** The interaction between the compound CCID24847856 and RBIVmcp. Left side indicate 3D interaction and the right portion indicates 2D interaction of the protein -ligands complex.

### ADME Analysis

The ADME analysis is an integral part of modern drug design and development processes which provides data associated with pharmacokinetics (PK). The analysis is capable of predicting the movement of drugs along with other physiochemical properties including water solubility, lipophilicity, medicinal chemistry, and medication likeness which is important in terms of developing a possible hypothesis for the selection of best drug candidates (Aljahdali et al., 2021). Moreover, before initiating preclinical studies on drugs, elucidating their pharmacophore features *insilico* can help to determine the xenobiotic properties of a compound. For this purpose, the Swiss-ADME server has been applied for the 3 selected ligand compounds. All of them had lipophilicity features, which suggested their potential to dissolve in oil, fat, and other non-polar solvents. Furthermore, the CCID5281855 and CCID1130 had high GI absorption rates. Other associated pharmacophore features also suggested that these 3 ligands can be "effective drug compounds" as illustrated in Table 2.

### Toxicity Prediction

In general, before the application of drug compounds their adverse effect on humans, other animals, plants, or to the outside environments need to be evaluated. Hence "toxicity prediction" has become an utmost important step for confirming a drug as safe-to-use compound (Raies & Bajic, 2016). The evaluation of a drug compound on an animal model requires massive time and effort, which is also an expensive process. However, on the other hand, predicting toxicity by computational approaches does not require an animal model, which is inexpensive and does not need a massive amount of time. In the present study, an *insilico* toxicity test conducted by ProTox-II tool revealed that 3 ligand compounds were non-toxic toward organisms which were further confirmed by hepatotoxicity, carcinogenicity, immunotoxicity, mutagenicity, and cytotoxicity values as described below in Table 3.

## Discussion

In recent times computer-aided drug design methods (CADDM) have been widely utilized to develop various products to accelerate the research associated with synthetic and biological fields (Yu & Mackerell, 2017). A well-established CADDMs can play an indispensable part in scientific research because they require low cost and time with a minimum amount of labor. Many synthetic compounds and natural phytochemical compounds have been identified as potential drug candidates against human and animal diseases such as Sars CoV, dengue, and WSSV by applying these well-established CADDMs (Qaddir et al., 2020; Nag, Paul, et al., 2021; Molla & Aljahdali, 2022). Selecting a highly suitable biologically active drug candidate against a specific disease-causing pathogen need to be validated through molecular docking and ADMET (chemical absorption, distribution, metabolism, excretion, and toxicity) analysis. Molecular docking helps to understand the mechanisms of the pathogenic molecule and how a particular drug candidate (ligand) interacts with pathogen-associated proteins (Aljahdali et al., 2021). Moreover, it clarifies the probable binding poses of a ligand and the protein which allows to identification most suitable drug candidates against the disease. Upon identification, conducting an ADMET analysis can further clarify the safe applicability of those drug candidates in the environment (Hadni & Elhallaoui, 2020).

The present study utilized a comprehensive computational drug design methodology to screen the *Trapa natans* phytochemicals against the Rock bream iridovirus major capsid protein ($RBIV_{mcp}$). A total of 13 phytochemicals compounds have been docked with the conserved active site region of the $RBIV_{mcp}$ that has the capacity to form diverse types of bonds and, depending on the binding affinity score three ligand-protein models were selected. The highest binding potentials have been observed for CCID5281855 (ellagic acid), CCID24847856 (galactoarabinan), and CCID1130 (thiamine) molecules with -5.1 kcal/mol, -6.4 kcal/mol, and -5.9 kcal/mol

**Table 2.** The pharmacokinetics and ADME properties of the 3 ligand compounds

| PROPERTIES | | CCID5281855 | CCID24847856 | CCID1130 |
|---|---|---|---|---|
| PHYSICOCHEMICAL ATTRIBUTE | Formula | $C_{14}H_6O_8$ | $C_{20}H_{36}O_{14}$ | $C_{12}H_{17}N4OS+$ |
| | MW (g/mol) | 302.19 g/mol | 500.49 g/mol | 265.35 g/mol |
| | Heavy atoms | 22 | 34 | 18 |
| | Aromatic heavy atoms | 16 | 0 | 11 |
| | Rotatable bonds | 2 | 8 | 4 |
| | H-bond acceptors | 8 | 14 | 3 |
| | H-bond donors | 4 | 7 | 2 |
| LIPOPHILICITY | Log Po/w | 1.31 | 1.99 | 2.54 |
| WATER SOLUBILITY | Log S (ESOL) | Soluble | Highly soluble | Soluble |
| PHARMACOKINETICS | GI absorption | High | Low | High |
| DRUG-LIKENESS | Lipinski | Yes | No | Yes |
| MEDI. CHEMISTRY | Synth. accessibility | Easy | Easy | Easy |

**Table 3.** List of the drug-induced toxicity properties includes hepatotoxicity, carcinogenicity, immunotoxicity, mutagenicity, cytotoxicity of 3 phytochemical compounds.

| PUBCHEM ID | HEPATOTOXICITY | CARCINOGENICITY | IMMUNOTOXICITY | MUTAGENICITY | CYTOTOXICITY |
|---|---|---|---|---|---|
| CCID5281855 | Inactive (0.83) | Inactive (0.84) | Inactive (0.81) | Inactive (0.84) | Inactive (0.9) |
| CCID24847856 | Inactive (0.93) | Inactive (0.81) | Lightly active (0.79) | Inactive (0.81) | Inactive (0.71) |
| CCID1130 | Inactive (0.89) | Inactive (0.52) | Inactive (0.95) | Inactive (0.87) | Inactive (0.64) |

respectively. The metabolite kinetics of these selected ligand compounds were analyzed *insilico* using the ADME, which is a straightforward method compared to the time-consuming conventional animal models (Yin et al., 2015; Aljahdali et al., 2021). Generally, ADME-associated pharmacokinetic properties need to be optimized before it is transferred to the standard pre-clinical trial as a suitable drug candidate (Wu et al., 2020). In the present study, 3 assessed phytochemical compounds had molecular weights and lipophilicities ranging from 265g/mol-500g/mol and 1.31-2.54 respectively. These two parameters are very important because having appropriate molecular weight can increase the permeability of a drug candidate whereas lipophilicity is the dissolving ability of a chemical compound in polar and non-polar solvents (Doak et al., 2014). Furthermore, having a high number of rotatable bonds and donor-acceptor hydrogen bonds are very important for the stimulation of membrane bilayer in-between crossing and to increase the oral bioavailability of a drug candidate (Veber et al., 2002). In the present study, galactoarabinan, ellagic acid, and thiamine had 2, 8, and 4 conventional and/or carbon-hydrogen bonds. Also, the amino acid 251 (GLU) in the acceptor showed to form bonds with all analyzed ligand compounds. Hence, these phytochemicals with low molecular weights, lipophilicities, and a high number of hydrogen bonds carry the potential to act as drug candidates against the $RBIV_{mcp}$.

Due to the development of technology, now researchers are capable of developing many drugs rapidly against diseases. However, it was suggested that around 40% of these drugs have been failed during the trials due to the positive ranges of toxicity (Doak et al., 2014; Kimmelman & Federico, 2017). A drug with high toxicity can generate adverse effects that can harm the organisms. Hence in the present study, *insilico* toxicity tests have been applied by utilizing the ProTox-II server to generate hepatotoxicity (possibility of chemical-driven liver damage), Carcinogenicity (potential of a substance that causes cancer), Immunotoxicity (possibility of causing adverse effects on the structure and/or function of the immune system), Mutagenicity (possibility of causing a mutation such as a change in the cell DNAs) and Cytotoxicity (possibility of chemical driven cell toxicity) parameters (Raies & Bajic, 2016; Banerjee et al., 2018). Among the ligand compounds, only ellagic acid and thiamine had low values than the required threshold in all toxicity parameters. Thiamine and their derivates previously proved to have beneficial effects against SARS-CoV and HIV with no side effects even when exposed to high doses whereas, ellagic acid has shown high inhibitory effects against human rhinoviruses ( Lu'o'ng & Ngyễn, 2013; Park et al., 2014; Al Sulaiman et al., 2021). The galactoarabinan compound in the present study had light immune toxicity. However, previous research suggested that this polysaccharide might have the potential to induce anticoagulative and immunomodulatory activities in organisms (Chang et al., 2021). Given this background, the present study suggests these 3 compounds can be assigned as potential antiviral drug candidates against the RBIV.

## Conclusion

Iridovirus in Rock bream aquaculture is a serious concern that has been affecting sustainable production in the Asian region during the past decade. The development of new antiviral candidates leading to the

control of RBIV is of adverse need to minimize the frequency of the virus infection. Therefore, the current study analyzed the binding mode of natural phytochemical compounds from *Trapa natans* against the major capsid protein of RBIV. This study combined CADDMs with homology modeling, molecular docking, ADME, and toxicity analysis, which revealed three potential antiviral drug candidates namely ellagic acid, galactoarabinan, and thiamine against the virus that might be able to prevent the activities of the $RBIV_{mcp}$. The orientation of the drug candidates in the active pocket region associated with their low binding energy against $RBIV_{mcp}$ makes them a preferential antiviral therapeutic agent against RBIV.

## Ethical Statement

Ethics not applicable.

## Funding Information

This research did not receive any specific grant from funding agencies in the public, commercial, or not-for-profit sectors.

## Author Contribution

First Author and Second Author: First two authors equally contributed to the contributed to the design, implementation, computational analysis of the results and to the writing of the manuscript; Third Author: Contributed to the writing, review & editing of the manuscript; and Fourth Author: Contributed to the writing, review & editing of the manuscript.

## Conflict of Interest

There is no conflict of interest. The authors declare that they have no known competing financial or non-financial, professional, or personal conflicts that could have appeared to influence the work reported in this paper.

## Acknowledgements

The first author conveys his thanks to all the members who participated in this research.

## References

Adkar, P., Dongare, A., Ambavade, S., & Bhaskar, V. H. (2014). *Trapa bispinosa* Roxb.: A review on nutritional and pharmacological aspects. Advances in Pharmacological Sciences, 2014. https://doi.org/10.1155/2014/959830

Ahammad, F., Abd Rashid, T. R. T., Mohamed, M., Tanbin, S., & Fuad, F. A. A. (2019). Contemporary Strategies and Current Trends in Designing Antiviral Drugs against Dengue Fever via Targeting Host-Based Approaches. Microorganisms 2019, Vol. 7, Page 296, 7(9), 296. https://doi.org/10.3390/Microorganisms7090296

Al Sulaiman, K., Aljuhani, O., Al Dossari, M., Alshahrani, A., Alharbi, A., Algarni, R., Al Jeraisy, M., Al Harbi, S., Al Katheri, A., Al Eidan, F., Al Bekairy, A. M., Al Qahtani, N., Al Muqrin, M., Vishwakarma, R., & Al Ghamdi, G. (2021). Evaluation of thiamine as adjunctive therapy in COVID-19 critically ill patients: a two-center propensity score matched study. Critical Care, 25(1), 1–8. https://doi.org/10.1186/S13054-021-03648-9/FIGURES/1

Aljahdali, M. O., Molla, M. H. R., & Ahammad, F. (2021). Compounds identified from marine mangrove plant (*Avicennia alba*) as potential antiviral drug candidates against WDSV, an in-silico approach. Marine Drugs, 19(5), 253. https://doi.org/10.3390/MD19050253/S1

Arya, A. K., Durgapal, M., Bachheti, A., Deepti, Joshi, K. K., Gonfa, Y. H., Bachheti, R. K., & Husen, A. (2022). Ethnomedicinal Use, Phytochemistry, and Other Potential Application of Aquatic and Semiaquatic Medicinal Plants. Evidence-Based Complementary and Alternative Medicine, 2022. https://doi.org/10.1155/2022/4931556

Banerjee, P., Eckert, A. O., Schrey, A. K., & Preissner, R. (2018). ProTox-II: a webserver for the prediction of toxicity of chemicals. Nucleic Acids Research, 46(W1), W257–W263. https://doi.org/10.1093/NAR/GKY318

Bateman, A., Martin, M. J., Orchard, S., Magrane, M., Agivetova, R., Ahmad, S., Alpi, E., Bowler-Barnett, E. H., Britto, R., Bursteinas, B., Bye-A-Jee, H., Coetzee, R., Cukura, A., da Silva, A., Denny, P., Dogan, T., Ebenezer, T. G., Fan, J., Castro, L. G., … Teodoro, D. (2021). UniProt: the universal protein knowledgebase in 2021. Nucleic Acids Research, 49(D1), D480–D489. https://doi.org/10.1093/NAR/GKAA1100

Brander, K. (2010). Reconciling biodiversity conservation and marine capture fisheries production. Current Opinion in Environmental Sustainability, 2(5–6), 416–421. https://doi.org/10.1016/J.COSUST.2010.09.003

Canuti, M., Large, G., Verhoeven, J. T. P., & Dufour, S. C. (2022). A Novel Iridovirus Discovered in Deep-Sea Carnivorous Sponges. Viruses, 14(8). https://doi.org/10.3390/v14081595

Chang, X., Shen, C. Y., & Jiang, J. G. (2021). Structural characterization of novel arabinoxylan and galactoarabinan from citron with potential antitumor and immunostimulatory activities. Carbohydrate Polymers, 269, 118331. https://doi.org/10.1016/J.CARBPOL.2021.118331

Chuang, H. C., Chu, T. W., Cheng, A. C., Chen, N. Y., & Lai, Y. S. (2022). Iridovirus isolated from marine giant sea perch causes infection in freshwater ornamental fish. Aquaculture, 548(P1), 737588. https://doi.org/10.1016/j.aquaculture.2021.737588

Colovos, C., & Yeates, T. O. (1993). Verification of protein structures: patterns of nonbonded atomic interactions. Protein Science : A Publication of the Protein Society, 2(9), 1511–1519. https://doi.org/10.1002/PRO.5560020916

Daina, A., Michielin, O., & Zoete, V. (2017). SwissADME: a free web tool to evaluate pharmacokinetics, drug-likeness and medicinal chemistry friendliness of small molecules. Scientific Reports 2017 7:1, 7(1), 1–13. https://doi.org/10.1038/srep42717

Dallakyan, S., & Olson, A. J. (2015). Small-molecule library screening by docking with PyRx. Methods in Molecular Biology (Clifton, N.J.), 1263, 243–250.

https://doi.org/10.1007/978-1-4939-2269-7_19

Do, J. W., Cha, S. J., Kim, J. S., An, E. J., Park, M. S., Kim, J. W., Kim, Y. C., Park, M. A., & Park, J. W. (2005). Sequence variation in the gene encoding the major capsid protein of Korean fish iridoviruses. Archives of Virology, 150(2), 351–359. https://doi.org/10.1007/S00705-004-0424-6

Do, J. W., Moon, C. H., Kim, H. J., Ko, M. S., Kim, S. B., Son, J. H., Kim, J. S., An, E. J., Kim, M. K., Lee, S. K., Han, M. S., Cha, S. J., Park, M. S., Park, M. A., Kim, Y. C., Kim, J. W., & Park, J. W. (2004). Complete genomic DNA sequence of rock bream iridovirus. Virology, 325(2), 351–363. https://doi.org/10.1016/j.virol.2004.05.008

Doak, B. C., Over, B., Giordanetto, F., & Kihlberg, J. (2014). Oral druggable space beyond the rule of 5: insights from drugs and clinical candidates. Chemistry & Biology, 21(9), 1115–1142. https://doi.org/10.1016/J.CHEMBIOL.2014.08.013

Dwevedi, A., Dwivedi, R., & Sharma, Y. (2016). Exploration of Phytochemicals Found in Terminalia sp. and their Antiretroviral Activities. Pharmacognosy Reviews, 10(20), 73–83. https://doi.org/10.4103/0973-7847.194048

Farooq, S., Atia-tul-Wahab, Choudhary, M. I., & Atta-ur-Rahman. (2023). Preventive Potential of Extracts of Some Dietary Plants against SARSCoV- 2 Infection. Current Traditional Medicine, 10(1). https://doi.org/10.2174/2215083809666230116141143

Fernández Sánchez, J. L., Le Breton, A., Brun, E., Vendramin, N., Spiliopoulos, G., Furones, D., & Basurco, B. (2022). Assessing the economic impact of diseases in Mediterranean grow-out farms culturing European sea bass. Aquaculture, 547, 737530. https://doi.org/10.1016/J.AQUACULTURE.2021.737530

Galluzzi, L., Brenner, C., Morselli, E., Touat, Z., & Kroemer, G. (2008). Viral Control of Mitochondrial Apoptosis. PLOS Pathogens, 4(5), e1000018. https://doi.org/10.1371/JOURNAL.PPAT.1000018

Guo, Z. (2017). The modification of natural products for medical use. Acta Pharmaceutica Sinica B, 7(2), 119–136. https://doi.org/10.1016/j.apsb.2016.06.003

Hadni, H., & Elhallaoui, M. (2020). 2D and 3D-QSAR, molecular docking and ADMET properties *in silico* studies of azaaurones as antimalarial agents. New Journal of Chemistry, 44(16), 6553–6565. https://doi.org/10.1039/C9NJ05767F

Heo, L., Park, H., & Seok, C. (2013). GalaxyRefine: protein structure refinement driven by side-chain repacking. Nucleic Acids Research, 41(W1), W384–W388. https://doi.org/10.1093/NAR/GKT458

Islam, S. I., Mou, M. J., Sanjida, S., & Mahfuj, S. (2022). An *In-silico* Approach for Identifying Phytochemical Inhibitors against Nervous Necrosis Virus (NNV) in Asian Sea Bass by Targeting Capsid Protein. Genetics of Aquatic Organisms, 6(2). https://doi.org/10.4194/GA487

Ito, T., Yoshiura, Y., Kamaishi, T., Yoshida, K., & Nakajima, K. (2013). Prevalence of red sea bream iridovirus among organs of Japanese amberjack (*Seriola quinqueradiata*) exposed to cultured red sea bream iridovirus. Journal of General Virology, 94(PART9), 2094–2101. https://doi.org/10.1099/VIR.0.052902-0/CITE/REFWORKS

Jung, M. H., Nikapitiya, C., Vinay, T. N., Lee, J., & Jung, S. J. (2017). Rock bream iridovirus (RBIV) replication in rock bream (*Oplegnathus fasciatus*) exposed for different time periods to susceptible water temperatures. Fish and Shellfish Immunology, 70, 731–735. https://doi.org/10.1016/j.fsi.2017.09.038

Kim, S., Chen, J., Cheng, T., Gindulyte, A., He, J., He, S., Li, Q., Shoemaker, B. A., Thiessen, P. A., Yu, B., Zaslavsky, L., Zhang, J., & Bolton, E. E. (2021). PubChem in 2021: new data content and improved web interfaces. Nucleic Acids Research, 49(D1), D1388–D1395. https://doi.org/10.1093/NAR/GKAA971

Kimmelman, J., & Federico, C. (2017). Consider drug efficacy before first-in-human trials. Nature 2017 542:7639, 542(7639), 25–27. https://doi.org/10.1038/542025a

Kurita, J., & Nakajima, K. (2012). Megalocytiviruses. Viruses, 4(4), 521–538. https://doi.org/10.3390/V4040521

Laskowski, R. A., Jabłońska, J., Pravda, L., Vařeková, R. S., & Thornton, J. M. (2018). PDBsum: Structural summaries of PDB entries. Protein Science : A Publication of the Protein Society, 27(1), 129–134. https://doi.org/10.1002/PRO.3289

Lin, J., Sahakian, D., de Morais, S., Xu, J., Polzer, R., & Winter, S. (2003). The role of absorption, distribution, metabolism, excretion and toxicity in drug discovery. Current Topics in Medicinal Chemistry, 3(10), 1125–1154. https://doi.org/10.2174/1568026033452096

Lu'o'ng, K. vinh quốc, & Ngyễn, L. T. H. (2013). The role of thiamine in HIV infection. International Journal of Infectious Diseases, 17(4), e221–e227. https://doi.org/10.1016/J.IJID.2012.11.019

Mohanraj, K., Karthikeyan, B. S., Vivek-Ananth, R. P., Chand, R. P. B., Aparna, S. R., Mangalapandi, P., & Samal, A. (2018). IMPPAT: A curated database of Indian Medicinal Plants, Phytochemistry and Therapeutics. Scientific Reports, 8(1), 1–17. https://doi.org/10.1038/s41598-018-22631-z

Molla, M. H. R., & Aljahdali, M. O. (2022). Identification of phytochemical compounds to inhibit the matrix-like linker protein VP26 to block the assembles of white spot syndrome virus (WSSV) envelope and nucleocapsid protein of marine shrimp: *In silico* approach. Journal of King Saud University - Science, 34(8), 102346. https://doi.org/10.1016/J.JKSUS.2022.102346

Monacelli, K., & Wilcox, D. A. (2021). Competition between two floating-leaved aquatic plants. Aquatic Botany, 172, 103390. https://doi.org/10.1016/J.AQUABOT.2021.103390

Mugimba, K. K., Byarugaba, D. K., Mutoloki, S., Evensen, Ø, & Munang'Andu, H. M. (2021). Challenges and Solutions to Viral Diseases of Finfish in Marine Aquaculture. Pathogens 2021, Vol. 10, Page 673, 10(6), 673. https://doi.org/10.3390/PATHOGENS10060673

Nag, A., Banerjee, R., & Roy, R. (2021). Phytochemicals as potential drug candidates for targeting SARS CoV 2 proteins, an *in silico* study. VirusDisease, 32(1), 98–107. https://doi.org/10.1007/s13337-021-00654-x

Nag, A., Paul, S., Banerjee, R., & Kundu, R. (2021). *In silico* study of some selective phytochemicals against a hypothetical SARS-CoV-2 spike RBD using molecular docking tools. Computers in Biology and Medicine, 137, 104818. https://doi.org/10.1016/J.COMPBIOMED.2021.104818

Naylor, R. L., Hardy, R. W., Buschmann, A. H., Bush, S. R., Cao, L., Klinger, D. H., Little, D. C., Lubchenco, J., Shumway, S. E., & Troell, M. (2021). A 20-year retrospective review of global aquaculture. Nature, 591(7851), 551–563. https://doi.org/10.1038/s41586-021-03308-6

Parekh, J., & Chanda, S. (2007). *In vitro* antimicrobial activity of *Trapa natans L.* fruit rind extracted in different solvents. African Journal of Biotechnology, 6(6), 766–770.

Park, S. W., Kwon, M. J., Yoo, J. Y., Choi, H. J., & Ahn, Y. J. (2014). Antiviral activity and possible mode of action of ellagic acid identified in *Lagerstroemia speciosa* leaves toward human rhinoviruses. BMC Complementary and Alternative Medicine, 14(1), 1–8. https://doi.org/10.1186/1472-6882-14-171

Qaddir, I., Majeed, A., Hussain, W., Mahmood, S., & Rasool, N. (2020). An *in silico* investigation of phytochemicals as potential inhibitors against non-structural protein 1 from dengue virus 4. Brazilian Journal of Pharmaceutical Sciences, 56, 1–21. https://doi.org/10.1590/S2175-97902020000117420

Raies, A. B., & Bajic, V. B. (2016). *In silico* toxicology: computational methods for the prediction of chemical toxicity. Wiley Interdisciplinary Reviews: Computational Molecular Science, 6(2), 147–172. https://doi.org/10.1002/WCMS.1240

Rani, A. C., Kalaimathi, K., Jayasree, S., Prabhu, S., Vijayakumar, S., Ramasubbu, R., & Priya, N. S. (2023). Exploring the Drug Potential of Phytochemicals as a Novel Therapeutic Drug Candidate for Herpesvirus: An *In-silico* Evaluation. Chemistry Africa, 6(2), 805–818. https://doi.org/10.1007/s42250-022-00529-8

Saxena, M. K., Neerja, S., Kumar, S., Mp, D., & Datta, S. (2021). Review potent pharmaceutical products from aquatic plants-Review. Pharmaceutical and Clinical Research, 14(1), 48-63. doi:10.22159/ajpcr.2021.v14i1.39992.

Seo, H., Kil, E. J., Fadhila, C., Vo, T. T. B., Auh, C. K., Lee, T. K., & Lee, S. (2020). Rapid diagnosis of two marine viruses, red sea bream iridovirus and viral hemorrhagic septicemia virus by PCR combined with lateral flow assay. VirusDisease, 31(3), 251–256. https://doi.org/10.1007/S13337-020-00577-Z/METRICS

Sohn, S.-G., Choi, D.-L., Do, J.-W., Hwang, J., & Park, J. (2000). Mass Mortalities of Cultured Striped Beakperch, *Oplegnathus fasciatus* by Iridoviral Infection. Journal of fish pathology, 13(2), 121-127. https://www.semanticscholar.org/paper/Mass-Mortalities-of-Cultured-Striped-Beakperch%2C-by-Sohn-Choi/47a691a98eebe13b6b8b841ad5d857b42b96250f

Stoicescu, I., Sirbu, R., Negreanu-Pirjol, T., Cociasu, M., Balaban, D. P., & Bala, C. (2012). *In Vitro* antioxidant and antibacterial activity of *Trapa Natans L.* aquatic plant from Danube delta area. Revue Roumaine de Chimie, 57(7–8), 729–733.

Subramaniam, K., Shariff, M., Omar, A. R., Hair-Bejo, M., & Ong, B. L. (2014). Detection and molecular characterization of infectious spleen and kidney necrosis virus from major ornamental fish breeding states in Peninsular Malaysia. Journal of Fish Diseases, 37(7), 609–618. https://doi.org/10.1111/JFD.12152

Tian, W., Chen, C., Lei, X., Zhao, J., & Liang, J. (2018). CASTp 3.0: Computed atlas of surface topography of proteins. Nucleic Acids Research, 46(W1), W363–W367. https://doi.org/10.1093/nar/gky473

Tidona, C. A., Schnitzler, P., Kehm, R., & Darai, G. (1998). Is the major capsid protein of iridoviruses a suitable target for the study of viral evolution? Virus Genes, 16(1), 59–66. https://doi.org/10.1023/A:1007949710031/METRICS

Veber, D. F., Johnson, S. R., Cheng, H. Y., Smith, B. R., Ward, K. W., & Kopple, K. D. (2002). Molecular properties that influence the oral bioavailability of drug candidates. Journal of Medicinal Chemistry, 45(12), 2615–2623. https://doi.org/10.1021/JM020017N/SUPPL_FILE/JM020017N_S.PDF

Walker, P. J., & Winton, J. R. (2010). Emerging viral diseases of fish and shrimp. Veterinary Research, 41(6). https://doi.org/10.1051/VETRES/2010022

Whittington, R. J., Becker, J. A., & Dennis, M. M. (2010). Iridovirus infections in finfish-critical review with emphasis on ranaviruses. Journal of Fish Diseases, 33(2), 95–122. https://doi.org/10.1111/j.1365-2761.2009.01110.x

Wiederstein, M., & Sippl, M. J. (2007). ProSA-web: interactive web service for the recognition of errors in three-dimensional structures of proteins. *Nucleic Acids Research, 35(suppl_2),* W407–W410. https://doi.org/10.1093/NAR/GKM290

Wu, F., Zhou, Y., Li, L., Shen, X., Chen, G., Wang, X., Liang, X., Tan, M., & Huang, Z. (2020). Computational Approaches in Preclinical Studies on Drug Discovery and Development. Frontiers in Chemistry, 8. https://doi.org/10.3389/FCHEM.2020.00726

Wu, Y. C., Kai, Y. H., & Chi, S. C. (2013). Persistently betanodavirus-infected barramundi (*Lates calcarifer*) exhibit resistances to red sea bream iridovirus infection. Developmental and Comparative Immunology, 41(4), 666–674. https://doi.org/10.1016/J.DCI.2013.06.011

Xu, D., & Zhang, Y. (2011). Improving the physical realism and structural accuracy of protein models by a two-step atomic-level energy minimization. Biophysical Journal, 101(10), 2525–2534. https://doi.org/10.1016/J.BPJ.2011.10.024

Yin, L., Zheng, L., Xu, L., Dong, D., Han, X., Qi, Y., Zhao, Y., Xu, Y., & Peng, J. (2015). *In-silico* prediction of drug targets, biological activities, signal pathways and regulating networks of dioscin based on bioinformatics. BMC Complementary and Alternative Medicine, 15(1), 1–17. https://doi.org/10.1186/S12906-015-0579-6/FIGURES/5

Yu, W., & Mackerell, A. D. (2017). Computer-aided drug design methods. Methods in Molecular Biology, 1520, 85–106. https://doi.org/10.1007/978-1-4939-6634-9_5

Zhang, Y. (2008). I-TASSER server for protein 3D structure prediction. BMC Bioinformatics, 9, 1–8. https://doi.org/10.1186/1471-2105-9-40

Zhou, X., Zhang, X., Han, Y., Jia, Q., & Gao, H. (2017). Vaccination with Recombinant Baculovirus Expressing Ranavirus Major Capsid Protein Induces Protective Immunity in Chinese Giant Salamander, *Andrias davidianus*. Viruses 2017, Vol. 9, Page 195, 9(8), 195. https://doi.org/10.3390/V9080195

Ziegler, S., Pries, V., Hedberg, C., & Waldmann, H. (2013). Target Identification for Small Bioactive Molecules: Finding the Needle in the Haystack. Angewandte Chemie International Edition, 52(10), 2744–2792. https://doi.org/10.1002/ANIE.201208749